Available online at www.sciencedirect.com
SCIENCE DIRECT®
Journal of Sound and Vibration 267 (2003) 29–55
JOURNAL OF SOUND AND VIBRATION
www.elsevier.com/locate/jsvi

Exact dynamic and static stiffness matrices of shear deformable thin-walled beam-columns

Kim Moon-Young[a,*], Kim Nam Il[a], Yun Hee-Taek[b]

[a] *Department of Civil-Environmental Engineering, SungKyunKwan University, Cheoncheon Dong Jangan-Ku, Kyoungki-Do, Suwon 440-746, South Korea*

[b] *Civil-Electric Research and Development Department, Korea Railroad Research Institute, Woulam-Dong, Kyonggi-Do, Uiwang-city 437-050, South Korea*

Received 14 May 2002; accepted 4 October 2002

Abstract

Total potential energy of non-symmetric thin-walled beam-columns in the general form is presented by introducing the displacement field based on semitangential rotations and deriving transformation equations between displacement and force parameters defined at the arbitrary axis and the centroid-shear center axis, respectively. Next, governing equations and force–deformation relations are derived from the total potential energy for a shear-deformable, uniform beam element and a system of linear eigenproblem with non-symmetric matrices is constructed based on 14 displacement parameters. And then explicit expressions for displacement parameters are derived and exact dynamic stiffness matrices are determined using force–deformatin relationships. In addition, the modified numerical method to eliminate multiple zero eigenvalues and to evaluate the exact static stiffness matrix is developed for spatial stability analysis. Finally, in order to demonstrate the validity and the accuracy of this study, the spatially coupled natural frequencies and buckling loads are evaluated and compared with analytical solutions or results analyzed by thin-walled beam elements and ABAQUS's shell elements.

1. Introduction

Recently, numerical methods that enable one to evaluate an exact dynamic element stiffness matrix for a beam element were proposed by many authors. Most of those studies adopted an analytical method, which exactly derived explicit expressions of displacement functions for governing equations. Friberg [1] evaluated an exact dynamic stiffness using Vlasov's equation for coupled vibration of beams. Banerjee [2] and Banerjee and Fisher [3] derived explicit expressions

*Corresponding author. Tel.: +82-31-290-7514; fax: +82-31-290-7548.
E-mail address: kmye@yurim.skku.ac.kr (K. Moon-Young).

0022-460X/03/$ - see front matter
doi:10.1016/S0022-460X(02)01410-4

for the coupled bending-torsional dynamic stiffness matrix of a uniform beam element. Leung [4] investigated the characteristic curves for lateral buckling of uniform beams under the constant bending moment using the dynamic stiffness. Afterwards, many researchers [5–8] derived the coupled bending-torsional dynamic stiffness for Timoshenko beam-column elements but did not account for shear-deformation effects due to restrained warping torsion of the non-symmetric cross-section. As Banerjee [9] pointed out, it is evident that those procedures can be easily developed by the help of symbolic computation and are very effective in saving the computing time due to the closed-form solution. These analytical methods, however, are sometimes inefficient because analytical operations in solving a system of simultaneous ordinary differential equations with many variables are so complex that those method may fail to yield the exact displacement functions.

On the other hand, Friberg [10] proposed the new numerical scheme based on the quadratic eigenproblem in calculating the exact dynamic stiffness matrix of thin-walled beam-columns and Leung and Zeng [11] presented a generalized formulation which is believed to improve Friberg's method. This method yields numerically exact displacement functions via a generalized linear eigenproblem with complex eigenvalues. But this method appears not to be general enough to solve the higher order simultaneous differential equation and may not give an exact static stiffness matrix owing to existence of multiple zero eigenvalues for a generalized eigenproblem.

The primary aim of the present paper is to develop an improved numerical procedure evaluating an exact dynamic and static stiffness matrix for the spatial free vibration and stability analysis of uniform and shear-deformable beams with non-symmetric thin-walled cross-sections. The important points presented are summarized as follows:

(1) Firstly, an improved theory considering the effects of shear deformations is developed for free vibration and stability of thin-walled beam-columns having non-symmetric cross-sections.
(2) Secondly, equations of motion and force–deformation relations are derived from the total potential energy of non-symmetric and shear-deformable thin-walled beams subjected to initial stress resultants based on semitangential rotations and semitangential moments [12].
(3) Thirdly, higher order simultaneous ordinary differential equations are transformed into the first order simultaneous differential equations by introducing 14 displacement parameters so that a generalized linear eigenvalue problem is obtained with non-symmetric matrices. Particularly in case of static problems, the efficient method of eliminate multiple zero eigenvalues for a generalized linear eigenproblem is devised by choosing 14 displacement parameters different from those of dynamic problems.
(4) And then using the solutions of the eigenproblem allowing the complex eigenvalues and eigenvectors, displacement functions of 14 displacement parameters are exactly derived with respect to nodal displacements.
(5) Finally, nodal forces are exactly evaluated using member force–deformation relationships and 14×14 dynamic and static element stiffness matrices are determined, where the Wittrick–Williams algorithm [13] is used to yield the natural frequencies.
(6) In order to demonstrate the validity and the accuracy of this procedure, the natural frequencies and buckling loads are evaluated and compared with analytical solutions or results of the analysis using beam elements and ABAQUS's shell elements [14] for the thin-walled straight beam structures.

2. An improved thin-walled beam-column theory

Displacement measures for a thin-walled cross-section with right-handed co-ordinate system observed from the positive x_1-axis are shown in Fig. 1. The x_1-axis is the member axis defined at an arbitrary point in the cross-section. x_2, x_3 axes are perpendicular to x_1 axis and these two axes need not be the principal inertia axes; U_x, U_y, U_z are rigid-body translations of the cross-section in the x_1, x_2 and x_3 direction, respectively; $\omega_1, \omega_2, \omega_3$ are rigid-body rotations about the x_1-, x_2- and x_3-axis, respectively; f is a parameter defining warping of the cross-section.

In this study, the right-body rotations $\omega_1, \omega_2, \omega_3$ are assumed as the semitangential rotations introduced by Argyris et al. [15,16]. The semitangential rotations have the commutative property independent of the (et al.) rotation sequence in the space, so the potential energy can be uniquely defined in the geometrically non-linear and stability analyses. Referring to the previous study by Kim and Kim [12], the displacement field including first and second order terms of the finite semitangential rotation may be written as

$$U_1(x_1,\ x_2,\ x_3) = U_x + \omega_2 x_3 - \omega_3 x_2 + f\phi, \tag{1a}$$

$$U_2(x_1,\ x_2,\ x_3) = U_y - \omega_1 x_3, \tag{1b}$$

$$U_3(x_1,\ x_2,\ x_3) = U_z + \omega_1 x_2 \tag{1c}$$

and

$$U_1^*(x_1,\ x_2,\ x_3) = \tfrac{1}{2}[\omega_1\omega_2 x_2 + \omega_1\omega_3 x_3], \tag{2a}$$

$$U_2^*(x_1,\ x_2,\ x_3) = \tfrac{1}{2}[-(\omega_1^2 + \omega_3^2)s_2 + \omega_2\omega_3 x_3], \tag{2b}$$

$$U_3^*(x_1,\ x_2,\ x_3) = \tfrac{1}{2}[\omega_2\omega_3 x_2 - (\omega_1^2 + \omega_2^2)x_3], \tag{2c}$$

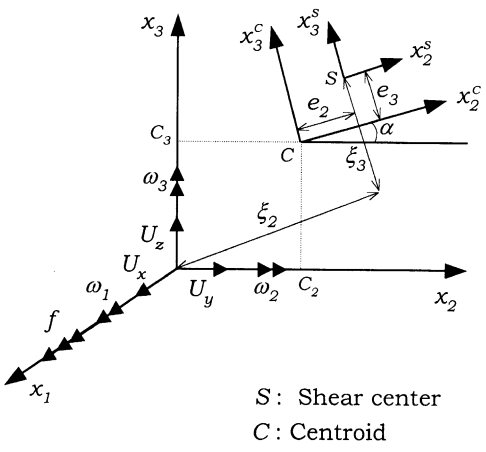

Fig. 1. Displacement parameters at the arbitrarily chosen axis.

where ϕ is the normalized warping function defined at the origin and satisfies a following relation for the warping function ϕ^s at the shear center

$$\phi = \phi^s - x_2^c \xi_3 + x_3^c \xi_2. \tag{3}$$

The three co-ordinate systems are used in this study (see Fig. 1). The (x_2, x_3)-axis is the arbitrarily chosen rectangular axis in the cross-section; $(x_2^c,\ x_3^c)$- and $(x_2^s,\ x_3^s)$-axis are defined at the centroid and the shear center, respectively, and coinciding with the direction of principal axes; c_2 and c_3 are co-ordinates of the centroid in (x_2, x_3) co-ordinate system; e_2 and e_3 are co-ordinates of the shear center in $(x_2^c,\ x_3^c)$ co-ordinate system; α is the angle between x_2^c and x_2 axis. The transformation between three co-ordinates systems is expressed as

$$x_2^c = x_2^s + e_2, \tag{4a}$$

$$x_3^c = x_3^s + e_3, \tag{4b}$$

and

$$x_2 = x_2^c \cos\alpha - x_3^c \sin\alpha + c_2, \tag{5c}$$

$$x_3 = x_2^c \cos\alpha - x_3^c \sin\alpha + c_3. \tag{5d}$$

Now, we define the cross-sectional constants defined at the arbitrary axis and the centroid-shear center, as follows:

$$\begin{aligned}
&S_2 = \int_A x_3 \,\mathrm{d}A = c_3 A, \quad S_3 = \int_A x_2 \,\mathrm{d}A = c_2 A, \quad S_\phi = \int_A \phi \,\mathrm{d}A = 0,\\
&I_2 = \int_A (x_3)^2 \,\mathrm{d}A, \quad I_3 = \int_A (x_2)^2 \,\mathrm{d}A, \quad I_{23} = \int_A x_2 x_3 \,\mathrm{d}A,\\
&I_{2\phi} = \int_A x_3 \phi \,\mathrm{d}A, \quad I_{3\phi} = \int_A x_2 \phi \,\mathrm{d}A, \quad I_\phi = \int_A \phi^2 \,\mathrm{d}A
\end{aligned} \tag{6}$$

and

$$\begin{aligned}
&S_2^c = \int_A x_3^c \,\mathrm{d}A = 0, \quad S_3^c = \int_A x_2^c \,\mathrm{d}A = 0, \quad S_\phi^s = \int_A \phi^s \,\mathrm{d}A = 0,\\
&I_2^c = \int_A (x_3^c)^2 \,\mathrm{d}A = 0, \quad I_3^c = \int_A (x_2^c)^2 \,\mathrm{d}A = 0, \quad I_{23}^c = \int_A x_2^c x_3^c \,\mathrm{d}A = 0,\\
&I_{2\phi}^s = \int_A x_3^c \phi^s \,\mathrm{d}A = 0, \quad I_{3\phi}^s = \int_A x_2^c \phi^s \,\mathrm{d}A = 0, \quad I_\phi^s = \int_A (\phi^s)^2 \,\mathrm{d}A = 0,
\end{aligned} \tag{7}$$

where the cross-sectional constants defined at $(x_2^c,\ x_3^c)$ and $(x_2^s,\ x_3^s)$ co-ordinate system are expressed using the right superscript 'c' and 's', respectively. These superscripts are also used for the definition of displacement parameters and stress resultants (see Fig. 2).

The transformation equations for the cross-sectional constants between three co-ordinate systems may be referred to the previous study by Kim and Kim [12]. For later use, ξ_2 and ξ_3 denote the distance from the origin of (x_2, x_3)-axis to the shear center in the direction of x_2^c- and

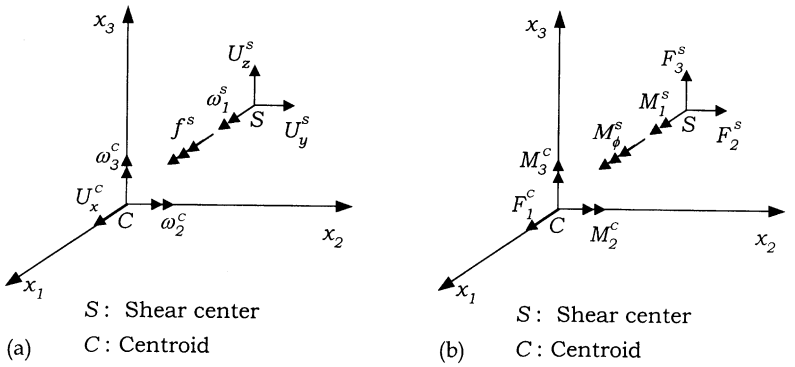

Fig. 2. Displacement parameters and stress resultants at the centroid-shear center: (a) Displacement parameters and (b) stress resultants.

x_3^c-axis, respectively, and are obtained as following:

$$\xi_2 = c_2 \cos\alpha + c_3 \sin\alpha + e_2, \tag{8a}$$

$$\xi_3 = -c_2 \sin\alpha + c_3 \cos\alpha + e_3. \tag{8b}$$

On the other hand, assuming that the in-plane strain measures are negligible according to the assumption of rigid deformation with respect to in-plane, stress resultants can be defined at the arbitrary axis and the centroid-shear center, respectively, as follows:

$$\begin{aligned}
&F_1 = \int_A \tau_{11}\,\mathrm{d}A, \quad F_2 = \int_A \tau_{12}\,\mathrm{d}A, \quad F_3 = \int_A \tau_{13}\,\mathrm{d}A,\\
&M_1 = \int_A (\tau_{13}x_2 - \tau_{12}x_3)\,\mathrm{d}A, \quad M_2 = \int_A \tau_{11}x_3\,\mathrm{d}A, \quad M_3 = -\int_A \tau_{11}x_2\,\mathrm{d}A,\\
&M_\phi = \int_A \tau_{11}\phi\,\mathrm{d}A, \quad M_R = \int_A \left(\tau_{12}\frac{\partial\phi}{\partial x_2} + \tau_3\frac{\partial\phi}{\partial x_3}\right)\mathrm{d}A, \quad M_P = \int_A \tau_{11}(x_2^2 + x_3^2)\,\mathrm{d}A
\end{aligned} \tag{9}$$

and

$$\begin{aligned}
&F_1^c = \int_A \tau_{11}\,\mathrm{d}A, \quad F_2^s = \int_A \tau_{12}^s\,\mathrm{d}A, \quad F_3^s = \int_A \tau_{13}^s\,\mathrm{d}A,\\
&M_1^s = \int_A (\tau_{13}^s x_2^s - \tau_{12}^s x_3^s)\,\mathrm{d}A, \quad M_2^c = \int_A \tau_{11}x_3^c\,\mathrm{d}A, \quad M_3^c = -\int_A \tau_{11}x_2^c\,\mathrm{d}A,\\
&M_\phi^s = \int_A \tau_{11}\phi^s\,\mathrm{d}A, \quad M_R^s = \int_A \left(\tau_{12}^s\frac{\partial\phi^2}{\partial x_2^s} + \tau_{13}^s\frac{\partial\phi^s}{\partial x_3^s}\right)\mathrm{d}A,\\
&M_P^s = \int_A \tau_{11}\{(x_2^s)^2 + (x_3^s)^2\}\,\mathrm{d}A,
\end{aligned} \tag{10}$$

where F_1, F_2 and F_3 are an axial force and shear forces, respectively; M_2 and M_3 are bending moments with respect to x_2- and x_3-axis, respectively; M_1 is the total twisting moments

with respect to the x_1-axis; M_R and M_ϕ are restrained (non-uniform) torsional moment and the bimoment about the x_1-axis, respectively; M_P is a stress resultant known as the Wagner effect and its detailed calculation procedure is given in the previous study of Kim and Kim [12].

In order to consistently obtain force–deformation relationships considering shear-deformation effects, transformation equations between displacement parameters and stress resultants defined at the arbitrary center (Fig. 1) and the centroid-shear center (Fig. 2), respectively, should be derived for non-symmetric thin-walled frame member. For this purpose, two force and displacement vectors composed of stress resultants and displacement parameters are defined by

$$\boldsymbol{F}^a = \langle F_1,\ F_2,\ F_3,\ M_1,\ M_2,\ M_3,\ M_\phi \rangle^{\mathrm{T}}, \tag{11a}$$

$$\boldsymbol{F}^s = \left\langle F_1^c,\ F_2^s,\ F_3^s,\ M_1^s,\ M_2^c,\ M_3^c,\ M_\phi^s \right\rangle^{\mathrm{T}}, \tag{11b}$$

and

$$\boldsymbol{D}^a = \langle U_x,\ U_y,\ U_z,\ \omega_1,\ \omega_2,\ \omega_3,\ f \rangle^{\mathrm{T}}, \tag{12a}$$

$$\boldsymbol{D}^s = \left\langle U_x^c,\ U_y^s,\ U_z^s,\ \omega_1^s,\ \omega_1^c,\ \omega_3^c,\ f^s \right\rangle^{\mathrm{T}}. \tag{12b}$$

Here stress resultant systems at the arbitrary center and those at the centroid-shear center Fig. 2(b), respectively, should be mechanically equivalent so that transformation equations between two force systems can be obtained by considering (3) as follows:

$$\begin{aligned}
F_1 &= F_1^c,\\
F_2 &= F_2^s \cos\alpha - F_3^s \sin\alpha,\\
F_3 &= F_2^s \sin\alpha + F_3^s \cos\alpha,\\
M_1 &= M_1^s - F_2^s\xi_3 + F_3^s\xi_2,\\
M_2 &= -M_3^c \sin\alpha + M_2^c \cos\alpha + c_3 F_1^c,\\
M_3 &= M_3^c \cos\alpha + M_2^c \sin\alpha - c_2 F_1^c,\\
M_\phi &= M_\phi^s + M_3^c\xi_3 + M_2^c\xi_2,\\
M_R &= M_R^s - F_2^s\xi_3 + F_3^s\xi_2.
\end{aligned} \tag{13a–h}$$

Then the principle of contragredience gets

$$(\boldsymbol{F}^a)^{\mathrm{T}}\boldsymbol{D}^a = (\boldsymbol{F}^s)^{\mathrm{T}}\boldsymbol{D}^s. \tag{14}$$

Now considering $\boldsymbol{F}^s$ as a virtual force vector and invoking the equilibrium condition (13), the resultant transformation between two displacement parameters (Figs. 1 and 2(a)) is

obtained as

$$\begin{gathered} U_x^c = U_x + c_3\omega_2 - c_2\omega_3, \\ U_y^s = U_y \cos\alpha + U_z \sin\alpha - \xi_3\omega_1, \\ U_z^s = -U_y \sin\alpha + U_z \cos\alpha + \xi_2\omega_1, \\ \omega_1^s = \omega_1, \\ \omega_2^c = \omega_2 \cos\alpha + \omega_3 \sin\alpha + f\xi_2, \\ \omega_3^c = -\omega_2 \sin\alpha + \omega_3 \cos\alpha + f\xi_3, \\ f^s = f. \end{gathered} \tag{15a–g}$$

On the other hand, referring to the study of Chang et al. [17], force–deformation relationships in the centroid-shear center formulation are given by

$$\begin{gathered} F_1^c = EAU_x^{c'}, \\ F_2^s = GA_2^s(U_y^{s'} - \omega_3^c), \\ F_3^s = GA_3^s\left(U_z^{s'} + \omega_2^c\right), \\ M_1^s - M_R^s = GJ\omega_1^{s'}, \\ M_R^s = GA_r^s(f^s + \omega_1^{s'}), \\ M_2^c = EI_2^c\omega_2^{c'}, \\ M_3^c = EI_3^c\omega_3^{c'}, \\ M_\phi^s = EI_\phi^s f^{s'}, \end{gathered} \tag{16a–h}$$

where E is the Young's modulus; J is the St. Venant torsion constant; G is the shear modulus; A_2^s, A_3^s and A_r^s are the effective shear areas defined by

$$\frac{1}{A_2^s} = \frac{1}{I_3^2}\int_A Q_3^2\frac{\mathrm{d}s}{t}, \quad \frac{1}{A_3^s} = \frac{1}{I_2^2}\int_A Q_2^2\frac{\mathrm{d}s}{t}, \quad \frac{1}{A_r^s} = \frac{1}{(I_\phi^s)^2}\int_A Q_r^2\frac{\mathrm{d}s}{t}, \tag{17a–c}$$

where

$$Q_2 = \int_0^s x_3 t\,\mathrm{d}s, \quad Q_3 = \int_0^s x_2 t\,\mathrm{d}s, \quad Q_r = \int_0^s \phi^s t\,\mathrm{d}s. \tag{18a–c}$$

Here, substituting Eqs. (15) and (16) into Eq. (13) and arranging leads to

$$\begin{aligned}
F_1 &= EAU_x' + ES_2\omega_2' - ES_3\omega_3',\\
F_2 &= GA_2(U_y' - \omega_3) + GA_{23}(U_z' + \omega_2) + GA_{2r}(\omega_1' + f),\\
M_3 &= EI_3\omega_3' - ES_3U_x' - EI_{23}\omega_2' - EI_{3\phi}f',\\
F_3 &= GA_3(U_z' + \omega_2) + GA_{23}(U_y' - \omega_3) + GA_{3r}(\omega_1' + f),\\
M_2 &= EI_2\omega_2' + ES_2U_x' - EI_{23}\omega_3' + EI_{2\phi}f',\\
M_1 - M_R &= GJ\omega_1',\\
M_R &= GA_r(\omega_1' + f) + GA_{2r}(U_y' - \omega_3) + GA_{3r}(U_z' + \omega_2),\\
M_\phi &= EI_\phi f' + EI_{2\phi}\omega_2' - EI_{3\phi}\omega_3',
\end{aligned} \tag{19a–h}$$

where

$$\begin{aligned}
A_2 &= A_2^s\cos^2\alpha + A_3^s\sin^2\alpha, \quad A_3 = A_3^s\cos^2\alpha + A_2^s\sin^2\alpha,\\
A_r &= A_r^s + A_2^s\xi_3^2 + A_3^2\xi_2^2, \quad A_{23} = (A_2^s + A_3^3)\cos\alpha\sin\alpha,\\
A_{2r} &= -A_2^s\xi_3\cos\alpha - A_3^s\xi_2\sin\alpha, \quad A_{3r} = -A_2^s\xi_3\sin\alpha + A_3^s\xi_2\cos\alpha.
\end{aligned} \tag{20a–f}$$

Here, it should be noticed that effects of the non-symmetric cross-section and shear deformations due to shear forces and restrained warping torsion are consistently take into account.

3. Equations of motion for a thin-walled beam column

The total potential energy of thin-walled space frame member (Π) is presented as

$$\Pi = \Pi_E + \Pi_G - \Pi_M - \Pi_{ext}, \tag{21}$$

where Π_M, Π_E, Π_G and Π_{ext} are the kinetic energy, the linear elastic energy, the potential energy due to the initial stress resultants and the potential energy corresponding to the element nodal forces, respectively. Each terms of the total potential energy (21) may be rewritten as

$$\Pi_E = \frac{1}{2}\int_L\int_A \tau_{ij}e_{ij}\,\mathrm{d}A\,\mathrm{d}x_1, \tag{22a}$$

$$\Pi_G = \int_L\int_A {}^0\tau_{ij}(\eta_{ij} + e_{ij}^*)\,\mathrm{d}A\,\mathrm{d}x_1, \tag{22b}$$

$$\Pi_M = \frac{1}{2}\omega^2\int_L\int_A \rho U_i^2\,\mathrm{d}A\,\mathrm{d}x_1, \tag{22c}$$

$$\Pi_{\mathrm{ext}} = \frac{1}{2}\int_s T_iU_i\,\mathrm{d}s, \tag{22d}$$

where e_{ij}, η_{ij} and e_{ij}^* are the conventional linear and non-linear strain due to U_i, the linear strain due to U_i^*, respectively, which are defined as follows:

$$e_{ij} = \tfrac{1}{2}(U_{i,j} + U_{j,i}), \tag{22f}$$

$$\eta_{ij} = \tfrac{1}{2}U_{i,k}U_{j,k}, \tag{22g}$$

$$e^*_{ij} = \tfrac{1}{2}(U^*_{i,j} + U^*_{j,i}), \tag{22h}$$

where the subscript 'comma' indicates partial differentiation with respect to the spatial coordinate (x_1, x_2, x_3).

Firstly, substituting the displacement field for the thin-walled space frame member into Eq. (22a) and noting definition equations of stress resultants, the elastic strain energy Π_E is reduced to the following expression:

$$\begin{aligned}\Pi_E = \frac{1}{2}\int_L [&F_1 U'_x + F_2(U'_y - \omega_3) + F_3(U'_3 + \omega_2) + M_2\omega'_2 \\ &+ M_3\omega'_3 + (M_1 - M_R)\omega'_1 + M_\phi f' + M_R(f + \omega'_1)]\,\mathrm{d}x_1.\end{aligned} \tag{23}$$

Finally, substituting Eq. (19) into Eq. (23) and rearranging, the elastic strain energy for non-symmetric thin-walled space frame member considering shear-deformation effects is derived as follows:

$$\begin{aligned}\Pi_E = \frac{1}{2}\int_L [&EAU'^2_x + EI_2\omega'^2_2 + EI_3\omega'^2_3 + GJ\omega'^2_1 + EI_\phi f'^2 \\ &+ 2ES_2U'_x\omega'_2 - 2ES_3U'_x\omega'_3 - 2EI_{23}\omega'_2\omega'_3 + 2EI_{2\phi}\omega'_2 f' - 2EI_{3\phi}\omega'_3 f' \\ &+ GA_2(U'_y - \omega_3)^2 + GA_3(U'_z + \omega_2)^2 + GA_r(\omega'_1 + f)^2 \\ &+ 2GA_{23}(U'_y - \omega_3)(U'_z + \omega_2) + 2GA_{2r}(U'_y - \omega_3)(\omega'_1 + f) \\ &+ 2GA_{3r}(U'_z + \omega_2)(\omega'_1 + f)]\,\mathrm{d}x_1.\end{aligned} \tag{24}$$

Also, the kinetic energy (Π_M), the potential energy due to the initial stress resultants (Π_G) and the potential energy corresponding to the element nodal forces (Π_{ext}) in (21) can be obtained by considering the displacement field, strain–displacement relations and the definition equations of stress resultants as follows:

$$\begin{aligned}\Pi_M = \frac{1}{2}\rho\omega^2\int_L [&A(U_x^2 + U_y^2 + U_z^2) + I_0\omega_1^2 + I_3\omega_3^2 + I_2\omega_2^2 + I_\phi f^2 \\ &+ 2S_2U_x\omega_2 - 2S_3U_x\omega_3 - 2I_{23}\omega_2\omega_3 + 2I_{2\phi}\omega_2 f \\ &- 2I_{3\phi}\omega_3 f + 2S_3U_z\omega_1 - 2S_2U_y\omega_1]\,\mathrm{d}x_1,\end{aligned} \tag{25}$$

$$\begin{aligned}\Pi_G = \frac{1}{2}\int_L [&{}^0F_1(U'^2_y + U'^2_z) + {}^0F_2(2U'_z\omega_1 + \omega_1\omega_2) - {}^0F_3(2U'_y\omega_1 - \omega_1\omega_3) \\ &+ {}^0M_2(\omega_1\omega'_3 - 2U'_y\omega'_1 + \omega'_1\omega_3) - {}^0M_3(\omega_1\omega'_2 + 2U'_z\omega'_1 + \omega'_1\omega_2) \\ &+ {}^0M_p\omega'^2_1 + {}^0M_1(\omega'_2\omega_3 - \omega_2\omega'_3)]\,\mathrm{d}x_1,\end{aligned} \tag{26}$$

$$\Pi_{ext} = \tfrac{1}{2}\boldsymbol{U}_e^{\mathrm{T}}\boldsymbol{F}_e. \tag{27}$$

The equations of motion and boundary conditions considering shear-deformation and rotary inertia effects can be obtained by substituting Eqs. (24)–(27) into Eq. (21) and invoking the variation principle.

In order to exactly evaluate dynamic stiffness, not only the cross-section of thin-walled beams should be uniform but also the initial stress resultants be constant. Hence in this study, it is assumed that the initial axial force is acted eccentrically so that axial force ${}^0F_1$, bending moments ${}^0M_2$,${}^0M_3$ are constant along the element axis, respectively, and initial torsional moment ${}^0M_1$ are also constant but initial shear forces and bimoment are zero. Now the equations of motion and geometric and natural boundary conditions are obtained by variation of (21) with respect to the seven displacement parameters as follows:

$$EAU_x'' + ES_2\omega_2'' - ES_3\omega_3'' + \rho\omega^2(AU_x + S_2\omega_2 - S_3\omega_3) = 0, \tag{28a}$$

$$\begin{aligned} &GA_2(U_y'' - \omega_3') + GA_{23}(U_z'' + \omega_2') + GA_{2r}(\omega_1'' + f') \\ &\quad + {}^0F_1U_y'' - {}^0M_2\omega_1'' + \rho\omega^2(AU_y - S_2\omega_1) = 0, \end{aligned} \tag{28b}$$

$$\begin{aligned} &GA_3(U_z'' + \omega_2') + GA_{23}(U_y'' - \omega_3') + GA_{3r}(\omega_1'' + f') \\ &\quad + {}^0F_1U_z'' - {}^0M_3\omega_1'' + \rho\omega^2(AU_z + S_3\omega_1) = 0, \end{aligned} \tag{28c}$$

$$\begin{aligned} &GJ\omega_1'' + GA_r(\omega_1'' + f') + GA_{2r}(U_y'' - \omega_3') + GA_{3r}(U_z'' + \omega_2') \\ &\quad - {}^0M_2U_y'' - {}^0M_3U_z'' + {}^0M_p\omega_1'' + \rho\omega^2(I_0\omega_1 + S_3U_z - S_2U_y) = 0, \end{aligned} \tag{28d}$$

$$\begin{aligned} &EI_2\omega_2'' + ES_2U_x'' - EI_{23}\omega_3'' + EI_{2\phi}f'' - GA_3(U_z' + \omega_2) - GA_{23}(U_y' - \omega_3) \\ &\quad - GA_{3r}(\omega_1' + f) + \rho\omega^2(I_2\omega_2 + S_2U_x - I_{23}\omega_3 + I_{2\phi}f) = 0, \end{aligned} \tag{28e}$$

$$\begin{aligned} &EI_3\omega_3'' - ES_3U_x'' - EI_{23}\omega_2'' - EI_{3\phi}f'' + GA_2(U_y' - \omega_3) + GA_{23}(U_z' + \omega_2) \\ &\quad + GA_{2r}(\omega_1' + f) + \rho\omega^2(I_3\omega_3 - S_3U_x - I_{23}\omega_2 - I_{3\phi}f) = 0, \end{aligned} \tag{28f}$$

$$\begin{aligned} &EI_\phi f'' + EI_{2\phi}\omega_2'' - EI_{3\phi}\omega_3'' - GA_r(\omega_1' + f) - GA_{2r}(U_y' - \omega_3) \\ &\quad - GA_{3r}(U_z' + \omega_2) + \rho\omega^2(I_\phi f + I_{2\phi}\omega_2 - I_{3\phi}\omega_3) = 0 \end{aligned} \tag{28g}$$

and

$$\delta U_x(o) = \delta U_x^p \text{ or } F_1(o) = -F_1^p, \quad \delta U_x(l) = \delta U_x^q \text{ or } F_1(l) = F_1^q, \tag{29a, b}$$

$$\delta U_y(o) = \delta U_y^p \text{ or } F_2(o) = -F_2^p, \quad \delta U_y(l) = \delta U_y^q \text{ or } F_2(l) = F_2^q, \tag{29c, d}$$

$$\delta U_z(o) = \delta U_z^p \text{ or } F_3(o) = -F_3^p, \quad \delta U_z(l) = \delta U_z^q \text{ or } F_3(l) = F_3^q, \tag{29e, f}$$

$$\delta\omega_1(o) = \delta\omega_1^p \text{ or } M_1(o) = -M_1^p, \quad \delta\omega_1(l) = \delta\omega_1^q \text{ or } M_1(l) = M_1^q, \tag{29g, h}$$

$$\delta\omega_2(o) = \delta\omega_2^p \text{ or } M_2(o) = -M_2^p, \quad \delta\omega_2(l) = \delta\omega_2^q \text{ or } M_2(l) = M_2^q, \tag{29i, j}$$

$$\delta\omega_3(o) = \delta\omega_3^p \text{ or } M_3(o) = -M_3^p, \quad \delta\omega_3(l) = \delta\omega_3^q \text{ or } M_3(l) = M_3^q, \tag{29k, l}$$

$$\delta f(o) = \delta f^p \text{ or } M_\phi(o) = -M_\phi^p, \quad \delta f(l) = \delta f^q \text{ or } M_\phi(l) = M_\phi^q, \tag{29m, n}$$

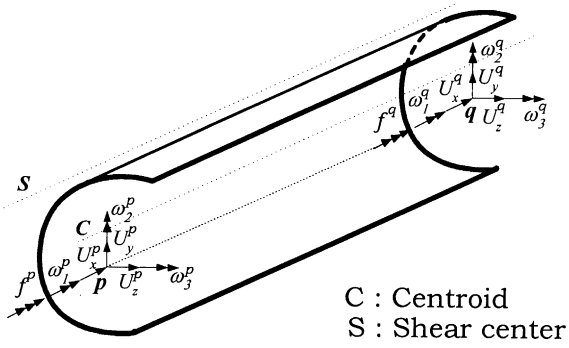

Fig. 3. Thin-walled beam-column element and its nodal displacements.

where superscripts 'p' and 'q' indicate end points of the member (see Fig. 3) and force–deformation relations are expressed as

$$F_1 = EAU_x' + ES_2\omega_2' - ES_3\omega_3', \tag{30a}$$

$$F_2 = GA_2(U_y' - \omega_3) + GA_{23}(U_z' + \omega_2) + GA_{2r}(\omega_1' + f) + {}^0F_1U_y' - {}^0M_2\omega_1', \tag{30b}$$

$$M_3 = EI_3\omega_3' - ES_3U_x' - EI_{23}\omega_2' - EI_{3\phi}f' + 0.5{}^0M_2\omega_1, \tag{30c}$$

$$F_3 = GA_3(U_z' + \omega_2) + GA_{23}(U_y' - \omega_3) + GA_{3r}(\omega_1' + f) + {}^0F_1U_z' - {}^0M_3\omega_1', \tag{30d}$$

$$M_2 = EI_2\omega_2' + ES_2U_x' - EI_{23}\omega_3' + EI_{2\phi}f' - 0.5{}^0M_3\omega_1, \tag{30e}$$

$$\begin{aligned} M_1 = {} & GJ\omega_1' + GA_r(\omega_1' + f) + GA_{2r}(U_y' - \omega_3) + GA_{3r}(U_z' + \omega_2) \\ & - {}^0M_2(U_y' - 0.5\omega_3) - {}^0M_3(U_z' + 0.5\omega_2) + {}^0M_p\omega_1', \end{aligned} \tag{30f}$$

$$M_\phi = EI_\phi f' + EI_{2\phi}\omega_2' - EI_{3\phi}\omega_3', \tag{30g}$$

where it should be noticed that Eq. (30) contains additional effects of initial forces when compared with Eq. (19). Also, it is evident that the equations of motion (28) constitute a set of the second order ordinary differential equation because of coupling effects of bending-torsional deformations and non-symmetry of the cross-section. In Sections 4 and 5, the new numerical method to evaluate an exact dynamic and static stiffness matrix of a thin-walled beam-column element with the non-symmetric section is developed by integrating the corresponding governing equations exactly.

4. Exact evaluation of dynamic element stiffness matrix

Firstly, in order to transform the higher order simultaneous ordinary differential equation (28) into simultaneous differential equations of the first order, a displacement state vector consisting of

14 displacement parameters is defined by

$$\begin{aligned}\boldsymbol{d}(x) &= \langle d_1,\ d_2,\ d_3,\ d_4,\ d_5,\ d_6,\ d_7,\ d_8,\ d_9,\ d_{10},\ d_{11},\ d_{12},\ d_{13},\ d_{14}\rangle^{\mathrm{T}} \\ &= \left\langle U_x,\ U_x',\ U_y,\ U_y',\ \omega_3,\ \omega_3',\ U_z,\ U_z',\ \omega_2,\ \omega_2',\ \omega_1,\ \omega_1',\ f,\ f'\right\rangle^{\mathrm{T}}. \end{aligned} \tag{31}$$

Now by rearranging Eq. (28) based on Eq. (31), the simultaneous ordinary differential equations of the first order with constant coefficients are obtained as follows:

$$d_1' = d_2, \tag{32a}$$

$$-EAd_2' + ES_3d_6' - ES_2d_{10}' = \rho\omega^2 Ad_1 - \rho\omega^2 S_3d_5 + \rho\omega^2 S_2d_9, \tag{32b}$$

$$d_3' = d_4, \tag{32c}$$

$$\begin{aligned}&-(GA_2 + {}^0F_1)d_4' - GA_{23}d_8' - (GA_{2r} - {}^0M_2)d_{12}' \\ &\quad = \rho\omega^2 Ad_3 - GA_2d_6 + GA_{23}d_{10} - \rho\omega^2 S_2d_{11} + GA_{2r}d_{14},\end{aligned} \tag{32d}$$

$$d_5' = d_6, \tag{32e}$$

$$\begin{aligned}ES_3d_2' - EI_3d_6' + EI_{23}d_{10}' + EI_{3\phi}d_{14}' &= -\rho\omega^2 S_3d_1 + GA_2d_4 - (GA_2 - \rho\omega^2 I_3)d_5 \\ &+ GA_{23}d_8 + (GA_{23} - \rho\omega^2 I_{23})d_9 + GA_{2r}d_{12} + (GA_{2r} - \rho\omega^2 I_{3\phi})d_{13},\end{aligned} \tag{32f}$$

$$d_7' = d_8, \tag{32g}$$

$$\begin{aligned}&-GA_{23}d_4' - (GA_3 + {}^0F_1)d_8' - (GA_{3r} - {}^0M_3)d_{12}' \\ &\quad = -GA_{23}d_6 + \rho\omega^2 Ad_7 + GA_3d_{10} + \rho\omega^2 S_3d_{11} + GA_{3r}d_{14},\end{aligned} \tag{32h}$$

$$d_9' = d_{10}, \tag{32i}$$

$$\begin{aligned}-ES_2d_2' + EI_{23}d_6' - EI_2d_{10}' - EI_{2\phi}d_{14}' &= \rho\omega^2 S_2d_1 - GA_{23}d_4 + (GA_{23} - \rho\omega^2 I_{23})d_5 \\ &- GA_3d_8 - (GA_3 - \rho\omega^2 I_2)d_9 - GA_{3r}d_{12} - (GA_{3r} - \rho\omega^2 I_{2\phi})d_{13},\end{aligned} \tag{32j}$$

$$d_{11}' = d_{12}, \tag{32k}$$

$$\begin{aligned}&-(GA_{2r} - {}^0M_2)d_4' - (GA_{3r} - {}^0M_3)d_8' - (GJ + GA_r + {}^0M_p)d_{12}' \\ &\quad = -\rho\omega^2 S_2d_3 - GA_{2r}d_6 + \rho\omega^2 S_3d_7 + GA_{3r}d_{10} + \rho\omega^2 I_0d_{11} + GA_rd_{14},\end{aligned} \tag{32l}$$

$$d_{13}' = d_{14}, \tag{32m}$$

$$\begin{aligned}EI_{3\phi}d_6' - EI_{2\phi}d_{10}' - EI_\phi d_{14}' &= -GA_{2r}d_4 + (GA_{2r} - \rho\omega^2 I_{3\phi})d_5 \\ &- GA_{3r}d_8 - (GA_{3r} - \rho\omega^2 I_{2\phi})d_9 - GA_rd_{12} - (GA_r - \rho\omega^2 I_\phi)d_{13},\end{aligned} \tag{32n}$$

which can be compactly expressed as

$$\boldsymbol{A}\boldsymbol{d}' = \boldsymbol{B}\boldsymbol{d}, \tag{33a}$$

where

$$\boldsymbol{A} = \left[\begin{array}{cccccc|cccccc}
k_1 & & & & & & & & & & & \\
 & k_2 & & & k_3 & & & k_4 & & & & \\
 & & k_1 & & & & & & & & & \\
 & & & k_5 & & & k_6 & & & k_7 & & \\
 & & & & k_1 & & & & & & & \\
 & k_3 & & & & k_8 & & k_9 & & & k_{10} & \\
 & & & & & & k_1 & & & & & \\
\hline
 & & & k_6 & & & k_{11} & & & k_{12} & & \\
 & & & & & & & k_1 & & & & \\
 & k_4 & & & k_9 & & & k_{13} & & & k_{14} & \\
 & & & & & & & & k_1 & & & \\
 & & & k_7 & & & k_{12} & & & k_{15} & & \\
 & & & & & & & & & & k_1 & \\
 & & & & k_{10} & & & k_{14} & & & k_{16} &
\end{array}\right], \tag{33b}$$

where

$$k_1 = 1.0, \quad k_2 = -EA, \quad k_3 = ES_3, \quad k_4 = -ES_2, \quad k_5 = -GA_2 - {}^0F_1, \quad k_6 = -GA_{23},$$
$$k_7 - GA_{2r} + {}^0M_2, \quad k_8 = -EI_3, \quad k_9 = EI_{23}, \quad k_{10} = EI_{3\phi}, \quad k_{11} = -GA_3 - {}^0F_1,$$
$$k_{12} = -GA_{3r} + {}^0M_3, \quad k_{13} = -EI_2, \quad k_{14} = -EI_{2\phi}, \quad k_{15} = -GJ - GA_r - {}^0M_p, \quad k = -EI_\phi,$$

$$\boldsymbol{B} = \left[\begin{array}{cccccc|cccccc}
 & b_1 & & & & & & & & & & \\
b_2 & & & & -b_3 & & & b_4 & & & & \\
 & & & b_1 & & & & & & & & \\
 & & b_2 & & & -b_5 & & & b_6 & -b_4 & & b_7 \\
 & & & & & b_1 & & & & & & \\
-b_3 & & & b_5 & b_8 & & b_6 & b_9 & & & b_7 & b_{10} \\
 & & & & & & b_1 & & & & & \\
\hline
 & & & & & -b_6 \quad b_2 & & & b_{11} & b_3 & & b_{12} \\
 & & & & & & & & b_1 & & & \\
b_4 & & & -b_6 & b_9 & & -b_{11} & b_{13} & & & -b_{12} & b_{14} \\
 & & & & & & & & & & b_1 & \\
 & & -b_4 & & & -b_7 \quad b_3 & & & b_{12} & b_{15} & & b_{16} \\
 & & & & & & & & & & & b_1 \\
 & & & -b_7 & b_{10} & & -b_{12} & b_{14} & & & -b_{16} & b_{17}
\end{array}\right], \tag{33c}$$

where

$$b_1 = 1.0, \quad b_2 = \rho\omega^2 A, \quad b_3 = \rho\omega^2 S_3, \quad b_4 = \rho\omega^2 S_2, \quad b_5 = GA_2, \quad b_6 = GA_{23},$$
$$b_7 = GA_{2r}, \quad b_8 = -GA_2 + \rho\omega^2 I_3, \quad b_9 = GA_{23} - \rho\omega^2 I_{23}, \quad b_{10} = GA_{2r} - \rho\omega^2 I_{3\phi},$$
$$b_{11} = GA_{3,} \quad b_{12} = GA_{3r}, \quad b_{13} = -GA_3 + \rho\omega^2 I_2, \quad b_{14} = -GA_{3r} + \rho\omega^2 I_{2\phi},$$
$$b_{15} = \rho\omega^2 I_0, \quad b_{16} = GA_r, \quad b_{17} = -GA_r + \rho\omega^2 I_\phi.$$

In order to find the general solution of Eq. (33a), the following eigenvalue problem is considered:

$$\lambda\, \boldsymbol{AZ} = \boldsymbol{BZ}, \tag{34}$$

where note that the matrix $\boldsymbol{A}$ is symmetric but $\boldsymbol{B}$ is non-symmetric. Hence, the eigensolution of Eq. (34) gives the eigenvalue and eigenvector with complex numbers. In this study, in order to resolve this problem, IMSL subroutine DGVCRG [18] is adopted so that eigensolutions of 14 pairs are calculated as follows:

$$(\lambda_i,\ \boldsymbol{Z}_i), \quad i = 1,\ 2, \ldots, 14, \tag{35}$$

where

$$\boldsymbol{Z}_i = \langle z_{1i},\ z_{2i},\ z_{3i},\ z_{4i},\ z_{5i},\ z_{6i},\ z_{7i},\ z_{8i},\ z_{9i},\ z_{10i},\ z_{11i},\ z_{12i},\ z_{13i},\ z_{14i},\rangle^{\mathrm{T}}.$$

Owing to the above eigensolution, the general solution of Eq. (33a) may be represented by the linear combination of eigenvectors with complex exponential functions as follows:

$$\boldsymbol{d}(x) = \sum_{i=1}^{14} a_i \boldsymbol{Z}_i e^{\lambda_i x} = \boldsymbol{X}(x)\boldsymbol{a} \tag{36}$$

and

$$\boldsymbol{X}(x) = [\boldsymbol{Z}_1 e^{\lambda_1 x};\ \boldsymbol{Z}_2 e^{\lambda_2 x};\ \boldsymbol{Z}_3 e^{\lambda_3 x};\ \boldsymbol{Z}_4 e^{\lambda_4 x};\ \boldsymbol{Z}_5 e^{\lambda_5 x};\ \boldsymbol{Z}_6 e^{\lambda_6 x};\ \boldsymbol{Z}_7 e^{\lambda_7 x};$$
$$\boldsymbol{Z}_8 e^{\lambda_8 x};\ \boldsymbol{Z}_9 e^{\lambda_9 x};\ \boldsymbol{Z}_{10} e^{\lambda_{10} x};\ \boldsymbol{Z}_{11} e^{\lambda_{11} x};\ \boldsymbol{Z}_{12} e^{\lambda_{12} x};\ \boldsymbol{Z}_{13} e^{\lambda_{13} x};\ \boldsymbol{Z}_{14} e^{\lambda_{14} x};\ ], \tag{37a}$$

$$\boldsymbol{a} = \langle a_1,\ a_2,\ a_3,\ a_4,\ a_5,\ a_6,\ a_7,\ a_8,\ a_9,\ a_{10},\ a_{11},\ a_{12},\ a_{13},\ a_{14}\rangle^{\mathrm{T}}. \tag{37b}$$

where $\boldsymbol{X}$ and $\boldsymbol{a}$ denote the 14×14 denote matrix function made up of 14 eigensolutions and the integration constant vector, respectively.

Now, it is necessary that complex coefficient vector $\boldsymbol{a}$ is represented with respect to 14 nodal displacement components (see Fig. 3). For this purpose, the nodal displacement vector is defined by

$$\boldsymbol{U}_e = \langle \boldsymbol{U}^p,\ \boldsymbol{U}^q \rangle^{\mathrm{T}}, \tag{38a}$$

$$\boldsymbol{U}^a = \left\langle u^a,\ v^a,\ \omega_3^a,\ w^a,\ \omega_2^a,\ \omega_1^a,\ f^a \right\rangle^{\mathrm{T}}, \quad \alpha = p,\ q, \tag{38b}$$

where

$$\boldsymbol{U}^p = \left\langle U_x(o),\ U_y(o),\ \omega_3(o),\ U_z(o),\ \omega_2(o),\ \omega_1(o),\ f(o) \right\rangle^{\mathrm{T}}, \tag{38c}$$

$$\boldsymbol{U}^q = \left\langle U_x(l),\ U_y(l),\ \omega_3(l),\ U_z(l),\ \omega_2(l),\ \omega_1(l),\ f(l) \right\rangle^{\mathrm{T}}. \tag{38d}$$

By substituting co-ordinates of the member end ($x = 0, l$) into Eq. (36) and accounting for Eq. (38), nodal displacement vector $\boldsymbol{U}_e$ can be obtained as follows:

$$\boldsymbol{U}_e = \boldsymbol{E}\boldsymbol{a}, \tag{39a}$$

where $\boldsymbol{E}$ is easily evaluated from $\boldsymbol{X}(\boldsymbol{x})$ and the detailed expression is

$$\boldsymbol{E} = \left[\begin{array}{ccccccc|ccccccc}
z_{1,1} & z_{1,2} & z_{1,3} & z_{1,4} & z_{1,5} & z_{1,6} & z_{1,7} & z_{1,8} & z_{1,9} & z_{1,10} & z_{1,11} & z_{1,12} & z_{1,13} & z_{1,14} \\
z_{3,1} & z_{3,2} & z_{3,3} & z_{3,4} & z_{3,5} & z_{3,6} & z_{3,7} & z_{3,8} & z_{3,9} & z_{3,10} & z_{3,11} & z_{3,12} & z_{3,13} & z_{3,14} \\
z_{5,1} & z_{5,2} & z_{5,3} & z_{5,4} & z_{5,5} & z_{5,6} & z_{5,7} & z_{5,8} & z_{5,9} & z_{5,10} & z_{5,11} & z_{5,12} & z_{5,13} & z_{5,14} \\
z_{7,1} & z_{7,2} & z_{7,3} & z_{7,4} & z_{7,5} & z_{7,6} & z_{7,7} & z_{7,8} & z_{7,9} & z_{7,10} & z_{7,11} & z_{7,12} & z_{7,13} & z_{7,14} \\
z_{9,1} & z_{9,2} & z_{9,3} & z_{9,4} & z_{9,5} & z_{9,6} & z_{9,7} & z_{9,8} & z_{9,9} & z_{9,10} & z_{9,11} & z_{9,12} & z_{9,13} & z_{9,14} \\
z_{11,1} & z_{11,2} & z_{11,3} & z_{11,4} & z_{11,5} & z_{11,6} & z_{11,7} & z_{11,8} & z_{11,9} & z_{11,10} & z_{11,11} & z_{11,12} & z_{11,13} & z_{11,14} \\
z_{13,1} & z_{13,2} & z_{13,3} & z_{13,4} & z_{13,5} & z_{13,6} & z_{13,7} & z_{13,8} & z_{13,9} & z_{13,10} & z_{13,11} & z_{13,12} & z_{13,13} & z_{13,14} \\
\hline
y_{1,1} & y_{1,2} & y_{1,3} & y_{1,4} & y_{1,5} & y_{1,6} & y_{1,7} & y_{1,8} & y_{1,9} & y_{1,10} & y_{1,11} & y_{1,12} & y_{1,13} & y_{1,14} \\
y_{3,1} & y_{3,2} & y_{3,3} & y_{3,4} & y_{3,5} & y_{3,6} & y_{3,7} & y_{3,8} & y_{3,9} & y_{3,10} & y_{3,11} & y_{3,12} & y_{3,13} & y_{3,14} \\
y_{5,1} & y_{5,2} & y_{5,3} & y_{5,4} & y_{5,5} & y_{5,6} & y_{5,7} & y_{5,8} & y_{5,9} & y_{5,10} & y_{5,11} & y_{5,12} & y_{5,13} & y_{5,14} \\
y_{7,1} & y_{7,2} & y_{7,3} & y_{7,4} & y_{7,5} & y_{7,6} & y_{7,7} & y_{7,8} & y_{7,9} & y_{7,10} & y_{7,11} & y_{7,12} & y_{7,13} & y_{7,14} \\
y_{9,1} & y_{9,2} & y_{9,3} & y_{9,4} & y_{9,5} & y_{9,6} & y_{9,7} & y_{9,8} & y_{9,9} & y_{9,10} & y_{9,11} & y_{9,12} & y_{9,13} & y_{9,14} \\
y_{11,1} & y_{11,2} & y_{11,3} & y_{11,4} & y_{11,5} & y_{11,6} & y_{11,7} & y_{11,8} & y_{11,9} & y_{11,10} & y_{11,11} & y_{11,12} & y_{11,13} & y_{11,14} \\
y_{13,1} & y_{13,2} & y_{13,3} & y_{13,4} & y_{13,5} & y_{13,6} & y_{13,7} & y_{13,8} & y_{13,9} & y_{13,10} & y_{13,11} & y_{13,12} & y_{13,13} & y_{13,14}
\end{array}\right], \tag{39b}$$

where $y_{i,j} = z_{i,j}e^{\lambda_i l}$, $i = 1, 3, 5, 7, 9, 11, 13$; $j = 1-14$ and the inverse of $\boldsymbol{E}$ is calculated using IMSL subroutine DLINCG [18].

Finally, elimination of the complex coefficient vector $\boldsymbol{a}$ from Eqs. (36) and (39a) yields the displacement state vector consisting of 14 displacement components

$$\boldsymbol{d}(\boldsymbol{x}) = \boldsymbol{X}(x)\boldsymbol{E}^{-1}\boldsymbol{U}_e. \tag{40}$$

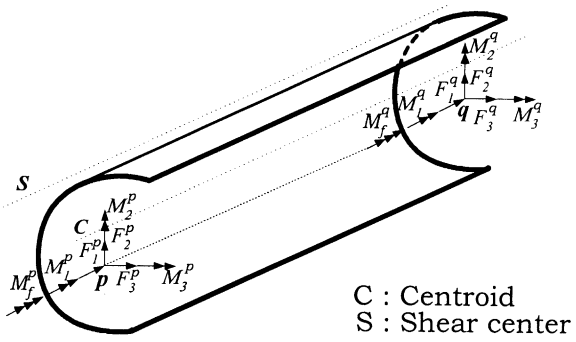

Fig. 4. Thin-walled beam-column element and its nodal forces.

Force–deformation relations of thin-walled beam columns have been derived in Section 3. For determination of exact dynamic stiffness matrix, nodal forces are depicted in Fig. 4 in which F_1, F_2, F_3 are axial force and shear forces, respectively. M_2, M_3 are bending moments, M_1, M_ϕ are torsional moment and bimoment and superscript p, q mean each ends of the member ($x = 0, l$). The nodal force vector is then defined by

$$\boldsymbol{F}_e = \langle \boldsymbol{F}^p,\ \boldsymbol{F}^q \rangle^{\mathrm{T}}, \tag{41a}$$

where

$$\boldsymbol{F}^\alpha = \left\langle F_1^\alpha,\ F_2^\alpha,\ M_3^\alpha,\ F_3^\alpha,\ M_2^\alpha,\ M_1^\alpha,\ M_\phi^\alpha \right\rangle^{\mathrm{T}}, \quad \alpha = p,\ q. \tag{41b}$$

From consideration of Eqs. (31), (30) can be rewritten as follows:

$$F_1 = EAd_2 - ES_3 d_6 + ES_2 d_{10}, \tag{42a}$$

$$F_2 = (GA_2 + {}^0F_1)d_4 - GA_2 d_5 + GA_{23} d_8 GA_{23} d_9 + (GA_{2r} - {}^0M_2)d_{12} + GA_{2r} d_{13}, \tag{42b}$$

$$M_3 = -ES_3 d_2 + EI_3 d_6 - EI_{23} d_{10} + 0.5{}^0M_2 d_{11} - EI_{3\phi} d_{14}, \tag{42c}$$

$$F_3 = GA_{23} d_4 - GA_{23} d_5 + (GA_3 + {}^0F_1)d_8 + GA_3 d_9 + (GA_{3r} - {}^0M_3)d_{12} + GA_{3r} d_{13}, \tag{42d}$$

$$M_2 = ES_2 d_2 - EI_{23} d_6 + EI_2 d_{10} - 0.5{}^0M_3 d_{11} + EI_{2\phi} d_{14}, \tag{42e}$$

$$\begin{aligned} M_1 = {} & (GA_{2r} - {}^0M_2)d_4 - (GA_{2r} - 0.5{}^0M_2)d_5 + (GA_{3r} - {}^0M_3)d_8 \\ & + (GA_{3r} - 0.5{}^0M_3)d_9 + (GJ + GA_r + {}^0M_p)d_{12} + GA_r d_{13}, \end{aligned} \tag{42f}$$

$$M_\phi = -EI_{3\phi} d_6 + EI_{2\phi} d_{10} + EI_\phi d_{14}, \tag{42g}$$

which is compactly represented as

$$\boldsymbol{f}(x) = \boldsymbol{S}\boldsymbol{d}(x), \tag{43a}$$

where $f = \langle F_1,\ F_2,\ M_3,\ F_3,\ M_2,\ M_1,\ M_\phi \rangle^{\mathrm{T}}$ and each element of 7×14 matrix $\boldsymbol{S}$ is

$$\boldsymbol{S} = \left[\begin{array}{cccc|cccccccc} s_1 & & & s_2 & & & s_3 & & & & & \\ & s_4 & s_5 & & s_6 & s_6 & & & s_7 & s_8 & & \\ s_2 & & & s_9 & & & s_{10} & s_{11} & & & s_{12} & \\ & s_6 & -s_6 & & s_{13} & s_{14} & & & s_{15} & s_{16} & & \\ s_3 & & & s_{10} & & & s_{17} & s_{18} & & & s_{19} & \\ & s_7 & s_{20} & & s_{15} & s_{21} & & & s_{22} & s_{23} & & \\ & & & s_{12} & & & s_{19} & & & & s_{24} & \end{array}\right], \tag{43b}$$

where

$$s_1 = EA, \quad s_2 = -ES_3, \quad s_3 = ES_2, \quad s_4 = GA_2 + {}^0F_1, \quad s_5 = -GA_2, \quad s_6 = GA_{23},$$
$$s_7 = GA_{2r} - {}^0M_2, \quad s_8 = GA_{2r}, \quad s_9 = EI_3, \quad s_{10} = -EI_{23}, \quad s_{11} = 0.5^0M_2,$$
$$s_{12} = -EI_{3\phi}, \quad s_{13} = GA_3 + {}^0F_1, \quad s_{14} = GA_3, \quad s_{15} = GA_{3r} - {}^0M_3,$$
$$s_{16} = GA_{3r}, \quad s_{17} = EI_2, \quad s_{18} = -0.5^0M_3, \quad s_{19} = EI_{2\phi}, \quad s_{20} = -GA_{2r} + 0.5^0M_2,$$
$$s_{21} = GA_{3r} - 0.5^0M_3, \quad s_{22} = GJ + GA_r + {}^0M_p, \quad s_{23} = GA_r, \quad s_{24} = EI_\phi.$$

Now substituting Eq. (40) into Eq. (43a) leads to

$$\boldsymbol{f}(\boldsymbol{x}) = \boldsymbol{SX}(\boldsymbol{x})\boldsymbol{E}^{-1}\boldsymbol{U}_e. \tag{44}$$

Also nodal forces at ends of element are evaluated as

$$\boldsymbol{F}^p = \boldsymbol{f}(\boldsymbol{o}) = -\boldsymbol{SX}(\boldsymbol{o})\boldsymbol{E}^{-1}\boldsymbol{U}_e, \tag{45a}$$

$$\boldsymbol{F}^q = \boldsymbol{f}(\boldsymbol{l}) = \boldsymbol{SX}(\boldsymbol{l})\boldsymbol{E}^{-1}\boldsymbol{U}_e. \tag{45b}$$

Consequently, the exact dynamic stiffness matrix $\boldsymbol{K}(\boldsymbol{\omega})$ of a thin-walled beam-column is calculated as follows:

$$\boldsymbol{F}_e = \boldsymbol{K}(\boldsymbol{\omega})\boldsymbol{U}_e, \tag{46a}$$

where

$$\boldsymbol{K}(\boldsymbol{\omega}) = \begin{bmatrix} -\boldsymbol{SX}(\boldsymbol{0})\boldsymbol{E}^{-1} \\ \boldsymbol{SX}(\boldsymbol{l})\boldsymbol{E}^{-1} \end{bmatrix}. \tag{46b}$$

Natural frequencies of thin-walled beam structures vibrating with the frequency ω under initial forces can be effectively determined by applying the Wittrick–Williams algorithm [13].

5. Evaluation method of exact static stiffness matrix

The circular frequency becomes zero in the equilibrium state. Therefore Eq. (28) is reduced to equilibrium equation (47) as follows:

$$EA\,U_x'' + ES_2\omega_2'' - ES_3\omega_3'' = 0, \tag{47a}$$

$$GA_2(U_y'' - \omega_3') + GA_{23}(U_z'' + \omega_2') + GA_{2r}(\omega_1'' + f') + {}^0F_1\,U_y'' - {}^0M_2\omega_1'' = 0, \tag{47b}$$

$$EI_3\omega_3'' - ES_3\,U_x'' - EI_{23}\omega_2'' - EI_{3\phi}\,f'' + GA_2(U_y' - \omega_3) + GA_{23}(U_z' + \omega_2) + GA_{2r}(\omega_1' + f) = 0, \tag{47c}$$

$$GA_3(U_z'' + \omega_2') + GA_{23}(U_y'' - \omega_3') + GA_{3r}(\omega_1'' + f') + {}^0F_1\,U_z'' - {}^0M_3\omega_1'' = 0, \tag{47d}$$

$$EI_2\omega_2'' + ES_2\,U_x'' - EI_{23}\omega_3'' + EI_{2\phi}\,f'' - GA_3(U_z' + \omega_2) - GA_{23}(U_y' - \omega_3) - GA_{3r}(\omega_1' + f) = 0, \tag{47e}$$

$$GJ\omega_1'' + GA_r(\omega_1'' + f') + GA_{2r}(U_y'' - \omega_3') + GA_{3r}(U_z'' + \omega_2') - {}^0M_2U_y'' - {}^0M_3U_z'' + {}^0M_p\omega_1'' = 0, \tag{47f}$$

$$EI_\phi f'' + EI_{2\phi}\omega_2'' - EI_{3\phi}\omega_3'' - GA_r(\omega_1' + f) - GA_{2r}(U_y' - \omega_3) - GA_{3r}(U_z' + \omega_2) = 0. \tag{47g}$$

In exactly integrating equilibrium equations of thin-walled beams, the evaluation procedure of the dynamic stiffness matrix cannot be directly applied to that of static stiffness due to existence of multiple zero eigenvalues from the associated eigenproblem. In order to eliminate multiple zero eigenvalues in advance, it is necessary to integrate the seven differential equations as follows:

$$\begin{aligned}
&U_x + S_2\omega_2/A - S_3\omega_3/A = a_1 + a_2x,\\
&GA_2(U_y' - \omega_3) + GA_{23}(U_z' + \omega_2) + GA_{2r}(\omega_1' + f) + {}^0F_1U_y' - {}^0M_2\omega_1' = a_6,\\
&EI_3\omega_3' - ES_3U_x' - EI_{23}\omega_2' - EI_{3\phi}f' - {}^0F_1U_y + {}^0M_2\omega_1 = a_5 - a_6x,\\
&GA_3(U_z' + \omega_2) + GA_{23}(U_y' - \omega_3) + GA_{3r}(\omega_1' + f) + {}^0F_1U_z' - {}^0M_3\omega_1' = a_{10},\\
&EI_2\omega_2' + ES_2U_x' - EI_{23}\omega_3' + EI_{2\phi}f' + {}^0F_1U_z - {}^0M_3\omega_1 = a_9 + a_{10}x,\\
&GJ\omega_1' + GA_r(\omega_1' + f) + GA_{2r}(U_y' - \omega_3) + GA_{3r}(U_z' + \omega_2)\\
&\quad - {}^0M_2U_y' - {}^0M_3U_z' + {}^0M_p\omega_1' = a_{14},\\
&EI_\phi f' + EI_{2\phi}\omega_2' - EI_{3\phi}\omega_3' + GJ\omega_1 - {}^0M_2U_y - {}^0M_3U_z + {}^0M_p\omega_1 = a_{13} + a_{14}x,
\end{aligned} \tag{48a–g}$$

where $a_i, i = 1, 2, 5, 6, 9, 10, 13, 14$ are the eight integration constants. From consideration of Eq. (48), the displacement state vector having 14 displacement parameters is defined by

$$\boldsymbol{d}(\boldsymbol{x}) = \langle d_1,\ d_2,\ d_3,\ d_4,\ d_5,\ d_6,\ d_7,\ d_8,\ d_9,\ d_{10},\ d_{11},\ d_{12},\ d_{13},\ d_{14}\rangle^{\mathrm{T}}. \tag{49}$$

where

$$\begin{aligned}
d_1 &= U_x + S_2\omega_2/A - S_3\omega_3/A,\\
d_2 &= U_x' + S_2\omega_2'/A - S_3\omega_3'/A,\\
d_3 &= U_y, \quad d_4 = \omega_3,\\
d_5 &= EI_3\omega_3' - ES_3U_x' - EI_{23}\omega_2' - EI_{3\phi}f' - {}^0F_1U_y + {}^0M_2\omega_1,\\
d_6 &= GA_2(U_y' - \omega_3) + GA_{23}(U_z' + \omega_2) + GA_{2r}(\omega_1' + f) + {}^0F_1U_y' - {}^0M_2\omega_1',\\
d_7 &= U_z, \quad d_8 = \omega_2,\\
d_9 &= EI_2\omega_2' + ES_2X_x' - EI_{23}\omega_3' + EI_{2\phi}f' + {}^0F_1U_z - {}^0M_3\omega_1,\\
d_{10} &= GA_3(U_z' + \omega_2) + GA_{23}(U_y' - \omega_3) + GA_{3r}(\omega_1' + f) + {}^0F_1U_z' - {}^0M_3\omega_1',\\
d_{11} &= \omega_1, \quad d_{12} = f,\\
d_{13} &= EI_\phi f' + EI_{2\phi}\omega_2' - EI_{3\phi}\omega_3' + GJ\omega_1 - {}^0M_2U_y - {}^0M_3U_z + {}^0M_p\omega_1,\\
d_{14} &= GJ\omega_1' + GA_r(\omega_1' + f) + GA_{2r}(U_y' - \omega_3) + GA_{3r}(U_z' + \omega_2)\\
&\quad - {}^0M_2U_y' - {}^0M_3U_z' + {}^0M_p\omega_1'.
\end{aligned} \tag{50a–n}$$

From Eqs. (48) and (49), the eight components of the displacement state vector $\boldsymbol{d}$ are evidently constant or linear function as follows:

$$\begin{aligned} d_1 &= a_1 + a_2 x; \quad d_2 = d_1' = a_2, \\ d_5 &= a_5 - a_6 x; \quad d_6 = -d_5' = a_6, \\ d_9 &= a_9 + a_{10} x; \quad d_{10} = d_9' = a_{10}, \\ d_{13} &= a_{13} + a_{14} x; \quad d_{14} = d_{13}' = a_{14}. \end{aligned} \tag{51a–h}$$

Based on Eq. (50), the simultaneous differential equation (48) may be rewritten as

$$(GA_2 + {}^0F_1)d_3' + GA_{23}d_7' + (GA_{2r} - {}^0M_2)d_{11}' = GA_2 d_4 - GA_{23}d_8 - GA_{2r}d_{12} + a_6, \tag{52a}$$

$$E(I_3 - S_3^2/A)d_4' - E(I_{23} - S_2S_3/A)d_8' - EI_{3\phi}d_{12}' = {}^0F_1 d_3 - {}^0M_2 d_{11} + a_5 + ES_3 a_2 - a_6 x, \tag{52b}$$

$$GA_{23}d_3' + (GA_3 + {}^0F_1)d_7' + (GA_{3r} - {}^0M_3)d_{11}' = GA_{23}d_4 - GA_3 d_8 - GA_{3r}d_{12} + a_{10}, \tag{52c}$$

$$\begin{aligned} &- E(I_{23} - S_2S_3/A)d_4' + E(I_2 - S_2^2/A)d_8' + EI_{2\phi}d_{12}' \\ &\quad = -{}^0F_1 d_7 + {}^0M_3 d_{11} + a_9 - ES_2 a_2 + a_{10} x, \end{aligned} \tag{52d}$$

$$\begin{aligned} &(GA_{2r} - {}^0M_2)d_3' + (GA_{3r} - {}^0M_3)d_7' + (GJ + GA_r + {}^0M_p)d_{11}' \\ &\quad = GA_{2r}d_4 - GA_{3r}d_8 - GA_r d_{12} + a_{14}, \end{aligned} \tag{52e}$$

$$-EI_{3\phi}d_4' + EI_{2\phi}d_8' + EI_\phi d_{12}' = {}^0M_2 d_3 + {}^0M_3 d_7 - (GJ + {}^0M_p)d_{11} + a_{13} + a_{14}x, \tag{52f}$$

which can be compactly expressed as

$$\boldsymbol{A}_s \boldsymbol{d}_s' = \boldsymbol{B}_s \boldsymbol{d}_s + \boldsymbol{C}, \tag{53}$$

where

$$\boldsymbol{d}_s(x) = \langle d_3,\ d_4,\ d_7,\ d_8,\ d_{11},\ d_{12},\ \rangle^{\mathrm{T}} = \langle U_y,\ \omega_3,\ U_z,\ \omega_2,\ \omega_1,\ f \rangle^{\mathrm{T}}, \tag{54a}$$

$$\boldsymbol{A}_s = \begin{bmatrix} g_1 & & g_2 & & g_3 & \\ & g_4 & & g_5 & & g_6 \\ g_2 & & g_7 & & g_8 & \\ & g_5 & & g_9 & & g_{10} \\ g_3 & & g_8 & & g_{11} & \\ & g_6 & & g_{10} & & g_{12} \end{bmatrix}, \quad \boldsymbol{B}_s = \begin{bmatrix} & b_1 & & b_2 & & b_3 \\ b_4 & & & & b_5 & \\ & -b_2 & & b_6 & & b_7 \\ & & -b_4 & & b_8 & \\ & -b_3 & & b_7 & & b_9 \\ -b_5 & & b_8 & & b_{10} & \end{bmatrix}, \tag{54b, c}$$

$$\boldsymbol{C} = \langle a_6,\ ES_3 a_2 + a_5 - a_6 x,\ a_{10}, -ES_2 a_2 + a_9 + a_{10} x,\ a_{14},\ a_{13} + a_{14} x \rangle^{\mathrm{T}}, \tag{54d}$$

where

$$g_1 = GA_2 + {}^0F_1, \quad g_2 = GA_{23}, \quad g_3 = GA_{2r} - {}^0M_2, \quad g_4 = E(I_3 - S_3^2/A),$$
$$g_5 = -E(I_{23} - S_2S_3/A), \quad g_6 = -EI_{3\phi}, \quad g_7 = GA_3 + {}^0F_1, \quad g_8 = GA_{3r} - {}^0M_3,$$
$$g_9 = E(I_2 - S_2^2/A), \quad g_{10} = EI_{2\phi}, \quad g_{11} = GJ + GA_r + {}^0M_p, \quad g_{12} = EI_\phi,$$
$$b_1 = GA_2, \quad b_2 = -GA_{23}, \quad b_3 = -GA_{2r}, \quad b_4 = {}^0F_1, \quad b_5 = -{}^0M_2,$$
$$b_6 = -GA_3, \quad b_7 = -GA_{3r}, \quad b_8 = {}^0M_3, \quad b_9 = -GA_r, \quad b_{10} = -GJ - {}^0M_p.$$

Clearly, Eq. (53) is the non-homogeneous simultaneous differential equation. When $\boldsymbol{C}$ is a zero vector, the procedure evaluating the homogeneous solution of Eq. (53) is similar to that of Section 4. Namely, the eigenproblem associated with Eq. (53) is given as

$$\lambda \boldsymbol{A}_s \boldsymbol{Z} = \boldsymbol{B}_s \boldsymbol{Z} \tag{55}$$

and, using IMSL subroutine DGVCRG [18], eigenvalues and eigenvectors of the six pairs are calculated in the complex domain.

$$(\lambda_i,\ \boldsymbol{Z}_i), \quad i = 1,\ 2, \ldots, 6, \tag{56}$$

where

$$\boldsymbol{Z}_i = \langle z_{1i},\ z_{2i},\ z_{3i},\ z_{4i},\ z_{5i},\ z_{6i} \rangle^{\mathrm{T}}.$$

Making use of Eq. (56), the homogeneous solution is expressible as linear combination with complex exponential functions as follows:

$$\boldsymbol{d}_s^{\boldsymbol{h}}(\boldsymbol{x}) = a_3\boldsymbol{Z}_1 e^{\lambda_1 x} + a_4\boldsymbol{Z}_2 e^{\lambda_2 x} + a_7\boldsymbol{Z}_3 e^{\lambda_3 x} + a_8\boldsymbol{Z}_4 e^{\lambda_4 x} + a_{11}\boldsymbol{Z}_5 e^{\lambda_5 x} + a_{12}\boldsymbol{Z}_6 e^{\lambda_6 x} = \boldsymbol{X}^{\boldsymbol{h}}(\boldsymbol{x})\boldsymbol{a}_{\boldsymbol{s}}, \tag{57}$$

where

$$\boldsymbol{X}^{\boldsymbol{h}}(\boldsymbol{x}) = [\boldsymbol{Z}_1 e^{\lambda_1 x};\ \boldsymbol{Z}_2 e^{\lambda_2 x};\ \boldsymbol{Z}_3 e^{\lambda_3 x};\ \boldsymbol{Z}_4 e^{\lambda_4 x};\ \boldsymbol{Z}_5 e^{\lambda_5 x};\ \boldsymbol{Z}_6 e^{\lambda_6 x}], \tag{58a}$$

$$\boldsymbol{a}_{\boldsymbol{s}} = \langle a_3,\ a_4,\ a_7,\ a_8,\ a_{11},\ a_{12} \rangle^{\mathrm{T}} \tag{58b}$$

and $\boldsymbol{X}^h$ and $\boldsymbol{a}_s$ denote the 6×6 matrix function made up of the six eigensolutions and the integration constant vector, respectively.

Next the particular solution $\boldsymbol{d}_s^p$ may be determined using the undetermined coefficient method. Noting that the vector $\boldsymbol{C}$ is the linear vector function, each components of $\boldsymbol{d}_s^p$ can be calculated as follows:

$$\boldsymbol{d}_s^p(\boldsymbol{x}) = (\boldsymbol{H} + \hat{\boldsymbol{H}}x)\boldsymbol{a}_c, \tag{59}$$

where

$$\boldsymbol{a}_c = \langle a_1,\ a_2,\ a_5,\ a_6,\ a_9,\ a_{10},\ a_{13},\ a_{14} \rangle^{\mathrm{T}}, \tag{60a}$$

$$\boldsymbol{H} = \boldsymbol{B}^{-1}[-\boldsymbol{A}\boldsymbol{B}^{-1}\boldsymbol{D}_2 - \boldsymbol{D}_1], \tag{60b}$$

$$\hat{\boldsymbol{H}} = -\boldsymbol{B}^{-1}\boldsymbol{D}_2, \tag{60c}$$

where

$$\boldsymbol{D}_1 = \begin{bmatrix} & & 1.0 & & & & \\ ES_3 & 1.0 & & & & & \\ & & & & 1.0 & & \\ -ES_2 & & & 1.0 & & & \\ & & & & & & 1.0 \\ & & & & & 1.0 & \end{bmatrix}, \quad \boldsymbol{D}_2 = \begin{bmatrix} & -1.0 & & & \\ & & & 1.0 & \\ & & & & 1.0 \end{bmatrix}. \tag{61a-b}$$

Resultantly, the general solution $\boldsymbol{d}_s$ is obtained by simply summing up the homogeneous solution (57) and the particular solution (59). Accordingly, the exact solution of the displacement state vector with respect to the integration constant vector $\boldsymbol{a}$ is constituted by solution (51) and the general solution $\boldsymbol{d}_s$

$$\boldsymbol{d}_s(x) = \boldsymbol{X}_s(x)\boldsymbol{a}, \tag{62}$$

where

$$\boldsymbol{X}_s = \left[\begin{array}{cccccccc|cccccccc} 1.0 & x & & & & & & & & & & & & & & \\ & 1.0 & & & & & & & & & & & & & & \\ h_{11}+\hat{h}_{11}x & h_{12}+\hat{h}_{12}x & x^h_{1,1} & x^h_{1,2} & h_{13}+\hat{h}_{13}x & h_{14}+\hat{h}_{14}x & x^h_{1,3} & & x^h_{1,4} & h_{15}+\hat{h}_{15}x & h_{16}+\hat{h}_{16}x & x^h_{1,5} & x^h_{1,6} & h_{17}+\hat{h}_{17}x & h_{18}+\hat{h}_{18}x \\ h_{21}+\hat{h}_{21}x & h_{22}+\hat{h}_{22}x & x^h_{2,1} & x^h_{2,2} & h_{23}+\hat{h}_{23}x & h_{24}+\hat{h}_{24}x & x^h_{2,3} & & x^h_{2,4} & h_{25}+\hat{h}_{25}x & h_{26}+\hat{h}_{26}x & x^h_{2,5} & x^h_{2,6} & h_{27}+\hat{h}_{27}x & h_{28}+\hat{h}_{28}x \\ & & & & 1.0 & -x & & & & & & & & & \\ & & & & & 1.0 & & & & & & & & & \\ h_{31}+\hat{h}_{31}x & h_{32}+\hat{h}_{32}x & x^h_{3,1} & x^h_{3,2} & h_{33}+\hat{h}_{33}x & h_{34}+\hat{h}_{34}x & x^h_{3,3} & & x^h_{3,4} & h_{35}+\hat{h}_{35}x & h_{36}+\hat{h}_{36}x & x^h_{3,5} & x^h_{3,6} & h_{37}+\hat{h}_{37}x & h_{38}+\hat{h}_{38}x \\ h_{41}+\hat{h}_{41}x & h_{42}+\hat{h}_{42}x & x^h_{4,1} & x^h_{4,2} & h_{43}+\hat{h}_{43}x & h_{44}+\hat{h}_{44}x & x^h_{4,3} & & x^h_{4,4} & h_{45}+\hat{h}_{45}x & h_{46}+\hat{h}_{46}x & x^h_{4,5} & x^h_{4,6} & h_{47}+\hat{h}_{47}x & h_{48}+\hat{h}_{48}x \\ \hline & & & & & & & & & 1.0 & x & & & & \\ & & & & & & & & & & 1.0 & & & & \\ h_{51}+\hat{h}_{51}x & h_{52}+\hat{h}_{52}x & x^h_{5,1} & x^h_{5,2} & h_{53}+\hat{h}_{53}x & h_{54}+\hat{h}_{54}x & x^h_{5,3} & & x^h_{5,4} & h_{55}+\hat{h}_{55}x & h_{56}+\hat{h}_{56}x & x^h_{5,5} & x^h_{5,6} & h_{57}+\hat{h}_{57}x & h_{58}+\hat{h}_{58}x \\ h_{61}+\hat{h}_{61}x & h_{62}+\hat{h}_{62}x & x^h_{6,1} & x^h_{6,2} & h_{63}+\hat{h}_{63}x & h_{64}+\hat{h}_{64}x & x^h_{6,3} & & x^h_{6,4} & h_{65}+\hat{h}_{65}x & h_{66}+\hat{h}_{66}x & x^h_{6,5} & x^h_{6,6} & h_{67}+\hat{h}_{67}x & h_{68}+\hat{h}_{68}x \\ & & & & & & & & & & & & & 1.0 & x \\ & & & & & & & & & & & & & & 1.0 \end{array}\right], \tag{63}$$

where $x^h_{i,j}$ and h_{ij} are elements of matrices $\boldsymbol{X}^h(x)$ and $\boldsymbol{H}$, respectively.

Now, it is necessary that the complex coefficient vector $\boldsymbol{a}$ is represented by 14 nodal displacement components. For this, substituting co-ordinates of the member end into Eq. (62) and arranging, the nodal displacement vector $\boldsymbol{U}_e$ is obtained as

$$\boldsymbol{U}_e = \boldsymbol{E}_s\boldsymbol{a}, \tag{64}$$

where

$$\boldsymbol{E}_s = \left[\begin{array}{ccccccc|ccccccc}
1.0 & & & & & & & & & & & & & \\
h_{11} & h_{12} & z_{1,1} & z_{1,2} & h_{13} & h_{14} & z_{1,3} & z_{1,4} & h_{15} & h_{16} & z_{1,5} & z_{1,6} & h_{17} & h_{18} \\
h_{21} & h_{22} & z_{2,1} & z_{2,2} & h_{23} & h_{24} & z_{2,3} & z_{2,4} & h_{25} & h_{26} & z_{2,5} & z_{2,6} & h_{27} & h_{28} \\
h_{31} & h_{32} & z_{3,1} & z_{3,2} & h_{33} & h_{34} & z_{3,3} & z_{3,4} & h_{35} & h_{36} & z_{3,5} & z_{3,6} & h_{37} & h_{38} \\
-h_{41} & -h_{42} & -z_{4,1} & -z_{4,2} & -h_{43} & -h_{44} & -z_{4,3} & -z_{4,4} & -h_{45} & -h_{46} & -z_{4,5} & -z_{4,6} & -h_{47} & -h_{48} \\
h_{51} & h_{52} & z_{5,1} & z_{5,2} & h_{53} & h_{54} & z_{5,3} & z_{5,4} & h_{55} & h_{56} & z_{5,5} & z_{5,6} & h_{57} & h_{58} \\
-h_{61} & -h_{62} & -z_{6,1} & -z_{6,2} & -h_{63} & -h_{64} & -z_{6,3} & -z_{6,4} & -h_{65} & -h_{66} & -z_{6,5} & -z_{6,6} & -h_{67} & -h_{68} \\
\hline
1.0 & l & & & & & & & & & & & & \\
h_{11}+\hat{h}_{11}l & h_{12}+\hat{h}_{12}l & y_{1,1} & y_{1,2} & h_{13}+\hat{h}_{13}l & h_{14}+\hat{h}_{14}l & y_{1,3} & y_{1,4} & h_{15}+\hat{h}_{15}l & h_{16}+\hat{h}_{16}l & y_{1,5} & y_{1,6} & h_{17}+\hat{h}_{17}l & h_{18}+\hat{h}_{18}l \\
h_{21}+\hat{h}_{21}l & h_{22}+\hat{h}_{22}l & y_{2,1} & y_{2,2} & h_{23}+\hat{h}_{23}l & h_{24}+\hat{h}_{24}l & y_{2,3} & y_{2,4} & h_{25}+\hat{h}_{25}l & h_{26}+\hat{h}_{26}l & y_{2,5} & y_{2,6} & h_{27}+\hat{h}_{27}l & h_{28}+\hat{h}_{28}l \\
h_{31}+\hat{h}_{31}l & h_{32}+\hat{h}_{32}l & y_{3,1} & y_{3,2} & h_{33}+\hat{h}_{33}l & h_{34}+\hat{h}_{34}l & y_{3,3} & y_{3,4} & h_{35}+\hat{h}_{35}l & h_{36}+\hat{h}_{36}l & y_{3,5} & y_{3,6} & h_{37}+\hat{h}_{37}l & h_{38}+\hat{h}_{38}l \\
-h_{41}-\hat{h}_{41}l & -h_{42}-\hat{h}_{42}l & -y_{4,1} & -y_{4,2} & -h_{43}-\hat{h}_{43}l & -h_{44}-\hat{h}_{44}l & -y_{4,3} & -y_{4,4} & -h_{45}-\hat{h}_{45}l & -h_{46}-\hat{h}_{46}l & -y_{4,5} & -y_{4,6} & -h_{47}-\hat{h}_{47}l & -h_{48}-\hat{h}_{48}l \\
h_{51}+\hat{h}_{51}l & h_{52}+\hat{h}_{52}l & y_{5,1} & y_{5,2} & h_{53}+\hat{h}_{53}l & h_{54}+\hat{h}_{54}l & y_{5,3} & y_{5,4} & h_{55}+\hat{h}_{55}l & h_{56}+\hat{h}_{56}l & y_{5,5} & y_{5,6} & h_{57}+\hat{h}_{57}l & h_{58}+\hat{h}_{58}l \\
-h_{61}-\hat{h}_{61}l & -h_{62}-\hat{h}_{62}l & -y_{6,1} & -y_{6,2} & -h_{63}-\hat{h}_{63}l & -h_{64}-\hat{h}_{64}l & -y_{6,3} & -y_{6,4} & -h_{65}-\hat{h}_{65}l & -h_{66}-\hat{h}_{66}l & -y_{6,5} & -y_{6,6} & -h_{67}-\hat{h}_{67}l & -h_{68}-\hat{h}_{68}l
\end{array}\right], \tag{65}$$

where $y_{i,j} = z_{i,j}e^{\lambda_j l}$, $i = 1,2,3,4,5,6$, $j = 1-6$ and the inverse of $\boldsymbol{E}$ is calculated using IMSL subroutine DLINCG [18].

Lastly, the static element stiffness matrix can be easily evaluated from Eq. (62) and force–deformation relations (30) by using the derivation procedures similar to those of Section 4. The final result of the static element stiffness matrix is

$$\boldsymbol{F}_e = \boldsymbol{K}_s \boldsymbol{U}_e, \tag{66a}$$

where

$$\boldsymbol{K}_s = \begin{bmatrix} -\boldsymbol{S}\boldsymbol{X}(\boldsymbol{0})\boldsymbol{E}^{-1} \\ \boldsymbol{S}\boldsymbol{X}(\boldsymbol{l})\boldsymbol{E}^{-1} \end{bmatrix}. \tag{66b}$$

Buckling loads of thin-walled beam structures can be determined by applying the condition that the determinant of static stiffness matrix is zero.

6. Numerical examples

In order to examine the validity and the accuracy of the proposed method, the spatial free vibration and stability analysis for the simply supported and cantilever thin-walled beam-columns are conducted and numerical results by the present study are compared with analytic solution and those by F.E. procedures using the thin-walled beam element and ABAQUS's shell element [14]. In case of finite element solutions using the beam element, the seven displacement parameters are interpolated by isoparametric shape functions corresponding to three-node element [20]. All geometric data are evaluated with respect to the centroid and principal axes except of effective shear areas.

6.1. Simply supported thin-walled beam-columns under an eccentrically axial force

In this example, spatially coupled free vibration and buckling problems of simply supported thin-walled beams under an eccentrically axial force are investigated. Material properties and

cross-sectional properties are listed below

$$E = 10\,000\ \mathrm{N/cm^2},\quad G = 5000\ \mathrm{N/cm^2},\quad A = 30\ \mathrm{cm^2},\quad J = 10\ \mathrm{cm^4},\quad L = 100\ \mathrm{cm},$$
$$I_2 = 100\ \mathrm{cm^4},\quad I_3 = 800\ \mathrm{cm^4},\quad I_\phi = 83\,750\ \mathrm{cm^6},\quad I_{2\phi} = 600\ \mathrm{cm^5},\quad I_{3\phi} = -800\ \mathrm{cm^5},$$
$$\rho = 0.00785\ \mathrm{kg/cm^3},\quad \beta_1 = 30\ \mathrm{cm^2},\quad \beta_2 = 25\ \mathrm{cm},\quad \beta_3 = -22\ \mathrm{cm},\quad A_2^s = 1\ \mathrm{cm^2},$$
$$A_3^s = 0.6\ \mathrm{cm^2},\quad A_r^s = 0.5\ \mathrm{cm^4},$$

where β_1, β_2, β_3 are the section parameters defined at the centroid and principal axes and their definition equations are given in the previous study of Kim et al. [19].

Here closed-form solutions for the simply supported thin-walled beam subjected to both the constant axial force and pure bending moments can be derived by using the harmonic functions [20] as follows:

$$U_y = A_n \sin\left(\frac{n\pi x}{L}\right)e^{i\omega t},\quad U_z = B_n \sin\left(\frac{n\pi x}{L}\right)e^{i\omega t},\quad \omega_1 = C_n \sin\left(\frac{n\pi x}{L}\right)e^{i\omega t}, \tag{67}$$

which corresponds to the assumption that the beam subdivides into n half sine waves during free vibration or buckling. Consequently, substitution of these expressions into the differential equations leads to a cubic equation for the critical values.

Table 1 shows that the coupled flexural-torsional frequencies by this study using a single element are presented and compared with the closed-form solution for a simply supported beam without and with an axial force. Note that the present solution coincide exactly with the closed-form solution. On the other hand, in Table 2, the coupled flexural–torsional buckling loads for a simply supported beam under an axial force at the shear center, the centroid, and the position $(\bar{x}_2,\ \bar{x}_3) = (-5\ \mathrm{cm},\ 7\ \mathrm{cm})$, respectively, are compared with the closed-form solution [19,20]. Clearly, Table 2 shows that the present solution using only a single element coincide exactly with the closed-form solution.

6.2. Thin-walled cantilever beams under an axial force

Fig. 5 shows a thin-walled cantilever beam subjected to an axial force at the centroid and its non-symmetric cross-section. For vibration and stability analysis, the material and geometric data are given as follows:

$$E = 30\,000\ \mathrm{N/cm^2},\quad G = 11\,500\ \mathrm{N/cm^2},\quad A = 8\ \mathrm{cm^2},\quad J = 0.6667\ \mathrm{cm^4},\quad L = 200\ \mathrm{cm},$$
$$I_2 = 114.872\ \mathrm{cm^4},\quad I_3 = 7.54463\ \mathrm{cm^4},\quad I_\phi = 408.333\ \mathrm{cm^6},\quad I_{2\phi} = 182.413\ \mathrm{cm^5},$$
$$I_{3\phi} = 18.9757\ \mathrm{cm^5},$$
$$\rho = 0.00785\ \mathrm{kg/cm^3},\quad \beta_1 = 15.3021\ \mathrm{cm^2},\quad \beta_2 = 0.57706\ \mathrm{cm},\quad \beta_3 = 5.93192\ \mathrm{cm},$$
$$A_2^s = 1.51452\ \mathrm{cm^2},\quad A_3^s = 4.46252\ \mathrm{cm^2},\quad A_r^s = 37.7520\ \mathrm{cm^4}.$$

Generally, it is not possible to derive closed-form solution for the spatially coupled vibration and stability analysis of the cantilever thin-walled beam subjected to an axial force. Thus, numerical

Table 1
Flexural–torsional natural frequencies under an axial force $(rad/s)^2$

Mode	Zero axial force		${}^0F_1 = -200\ N$ at $(\bar{x}_2,\ \bar{x}_3) = (-5,\ 7)$	
	Present study	Analytic solution [20]	Present study	Analytic solution [20]
	1.09513	1.09513	0.198424	0.198424
$n=1$	4.01706	4.01706	3.64734	3.64734
	63.1947	63.1947	60.1912	60.1912
	4.80932	4.80932	1.57140	1.57140
$n=2$	33.8270	33.8270	31.7785	31.7785
	362.287	362.287	350.396	350.396
	11.0357	11.0357	3.90529	3.90529
$n=3$	97.4077	97.4077	92.3298	92.3298
	900.027	900.027	873.450	873.450

Table 2
Flexural–torsional buckling loads under an axial force P (N)

Mode	At shear center		At centroid		At $(\bar{x}_2,\ \bar{x}_3) = (-5,\ 7)$	
	Present study	Analytic solution [20]	Present study	Analytic solution [20]	Present study	Analytic solution [20]
	184.528	184.528	261.338	261.338	242.156	242.156
$n=1$	742.641	742.641	960.533	960.533	2511.28	2511.28
	3061.37	3061.37	15375.5	15375.5	9066.84	9066.84

solutions analyzed by this study are compared with those by 12 thin-walled isoparametric beam elements and 600 shell elements using nine-noded shell element (S9R5) of ABAQUS. Tables 3 and 4 show that flexural–torsional natural frequencies and buckling loads by this study are well compared with those by two finite element methods. It is evident that numerical results by this study using a single element are in a good agreement with those by ABAQUS's shell element as well as the thin-walled beam element.

7. Conclusions

A general formulation for spatial free vibration and stability analysis of non-symmetric thin-walled space frame member considering the effects of shear deformations was presented based on the displacement parameters defined at the arbitrarily chosen axis, including second order terms of finite semitangential rotations. For the exact evaluation of a dynamic and static element stiffness matrix for a uniform and shear-deformable beam-column element with non-symmetric thin-walled cross-section, equations of motion is firstly transformed into the first order differential

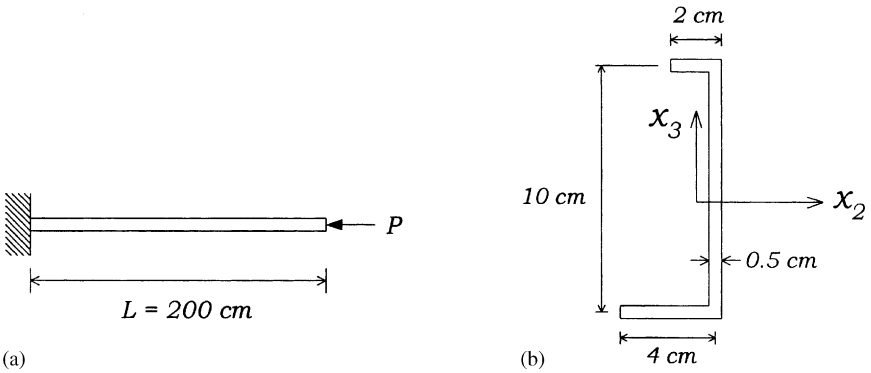

Fig. 5. Cantilever beam with non-symmetric channel section: (a) Cantilever beam under an axial force and (b) non-symmetric channel section.

Table 3
Flexural–torsional natural frequencies for the cantilever beam $(rad/s)^2$

Mode	Present study	Three-node beam elements	ABAQUS
1	0.027	0.027	0.028
2	0.334	0.335	0.331
3	0.704	0.704	0.696
4	1.065	1.065	1.074
5	4.817	4.818	4.766
6	7.055	7.060	7.083
7	17.86	17.89	17.95
8	19.30	19.32	19.36
9	23.74	23.78	23.58
10	45.71	46.08	46.52

Table 4
Flexural–torsional buckling loads for cantilever under axial force at centroid (N)

Mode	Present study	Three-node beam elements	ABAQUS
1	13.789	13.789	14.001
2	111.84	111.85	113.10
3	191.16	191.16	190.08
4	255.10	255.20	256.67
5	406.28	406.79	408.53

equations and a generalized linear eigenproblem having complex eigenvalues is considered. In case of static problems, the efficient method to eliminate multiple zero eigenvalues for a generalized linear eigenproblem is devised by choosing 14 displacement parameters different from those of

dynamic problems. Then displacement functions are exactly derived and dynamic element stiffness matrices are determined using member force-deformation relationships. Finally, it is demonstrated that numerical results by the present method are in a good agreement with those using both thin-walled beam elements and ABAQUS's shell element. Resultantly, it is believed that the present procedure is general and provides a systematic tool for the numerical evaluation of dynamic and static stiffness matrices for a shear-deformable beam-column element.

Acknowledgements

The authors are grateful for the support provided by a grant (E00511) from the Korea Research Foundation (KRF).

References

[1] P.O. Friberg, Coupled vibrations of beams—an exact dynamic element stiffness matrix, International Journal for Numerical Methods in Engineering 19 (1983) 479–493.
[2] J.R. Banerjee, Coupled bending-torsional dynamic stiffness matrix for beam elements, International Journal for Numerical Methods in Engineering 28 (1989) 1283–1298.
[3] J.R. Banerjee, S.A. Fisher, Coupled bending-torsional dynamic stiffness matrix for axially loaded beam elements, International Journal for Numerical Methods in Engineering 33 (1992) 739–751.
[4] A.Y.T. Leung, Dynamic stiffness for lateral buckling, Computers and Structures 42 (3) (1992) 321–325.
[5] J.R. Banerjee, F.W. Williams, Coupled bending-torsional dynamic stiffness matrix for Timoshenko beam elements, Computers and Structures 42 (3) (1992) 301–310.
[6] J.R. Banerjee, F.W. Williams, Coupled bending-torsional dynamic stiffness matrix of an axially loaded Timoshenko beam element, International Journal of Solids and Structures 31 (6) (1994) 749–762.
[7] J.R. Banerjee, F.W. Williams, Exact dynamic stiffness matrix for composite Timoshenko beams with applications, Journal of Sound and Vibration 194 (4) (1996) 573–585.
[8] J.R. Banerjee, Free vibration of axially loaded composite Timoshenko beams using the dynamic stiffness matrix method, Computers and Structures 69 (1998) 197–208.
[9] J.R. Banerjee, Dynamic stiffness formulation for structural elements: a general approach, Computers and Structures 63 (1) (1997) 101–103.
[10] P.O. Friberg, Beam element matrices derived from Vlasov's theory of open thin-walled elastic beams, International Journal for Numerical Methods in Engineering 21 (1985) 1205–1228.
[11] A.Y.T. Leung, S.P. Zeng, Analytical formulation of dynamic stiffness, Journal of Sound and Vibration 177 (4) (1994) 555–564.
[12] S.B. Kim, M.Y. Kim, Improved formulation for spatial stability and free vibration of thin-walled tapered beams and space frames, Engineering Structures 22 (2000) 446–458.
[13] W.H. Wittrick, F.W. Williams, A general algorithm for computing natural frequencies of elastic structures, The Quarterly Journal of Mechanics and Applied Mathematics 24 (1971) 263–284.
[14] ABAQUS 1992 User's Manual Vols. I and II, Ver. 5.2. Hibbit, Karlsson & Sorensen, Inc.
[15] J.H. Argyris, P.C. Dunne, D.W. Scharpf, On large displacement–small strain analysis of structures with rotational degrees of freedom, Computer Methods in Applied Mechanics and Engineering 14 (1978) 401–451.
[16] J.H. Argyris, P.C. Dunne, G. Malejannakis, D.W. Scharpf, On large displacement-small strain analysis of structures with rotational degrees of freedom (continued form), Computer Methods in Applied Mechanics and Engineering 15 (1978) 99–135.
[17] S.P. Chang, S.B. Kim, M.Y. Kim, Stability of shear deformable thin-walled space frames and circular arches, Journal of Engineering and Mechanics American Society of Civil Engineers 122 (9) (1996) 844–854.

[18] Microsoft IMSL Library 1995. Microsoft Corporation.
[19] M.Y. Kim, S.P. Chang, S.B. Kim, Spatial stability and free vibration of shear flexible thin-walled elastic beams I: analytical approach, International Journal for Numerical Methods in Engineering 37 (1994) 4097–4115.
[20] M.Y. Kim, S.P. Chang, S.B. Kim, Spatial stability and free vibration of shear flexible thin-walled elastic beams II: numerical approach, International Journal for Numerical Methods in Engineering 37 (1994) 4117–4140.